Int. J. Heat Mass Transfer. Vol. 29, No. 2, pp. 317–329, 1986
Printed in Great Britain

0017–9310/86 $3.00 + 0.00
Pergamon Press Ltd.

An integral solution of moving boundary problems

M. MASHENA† and A. HAJI-SHEIKH
Mechanical Engineering Department, University of Texas at Arlington, Arlington, TX 76019, U.S.A.

(*Received* 12 *June* 1984 *and in final form* 9 *September* 1985)

Abstract—An integral method is presented that utilizes Galerkin functions and leads to closed-form solutions for temperature distribution in the liquid and solid phase. Unlike methods using quasi-steady assumptions, this method retains the contribution of the internal heat capacity of solid and liquid, therefore, accommodating problems involving time-dependent temperature along the boundary. The method is applied to classical one- and two-dimensional solidification problems to test its accuracy. The agreement between this method and the existing one-dimensional boundary-layer integral method is excellent. The two-dimensional results for a square geometry are compared to the experimental data obtained for octadecane.

INTRODUCTION

AMONG NUMEROUS numerical and analytical treatments of moving boundary problems cited in the literature, one-dimensional geometries have received considerably more attention. Numerical methods are primarily used for two- and three-dimensional bodies. The numerical solutions can be classified into two categories: the single-region approach and the multiple-region approach. In the single-region approach, which is also known as the enthalpy or heat capacity method, the energy equation is applied once over the entire liquid and solid regions and the latent energy release is simulated by modifying the specific heat or enthalpy. In the multiple-region approach the energy equation is applied separately for each phase and the two equations are coupled using energy balance in addition to the continuity of temperature at the interface.

Some of the solution methods used for one-dimensional geometries with moving boundaries are the approximate integral method [1–3], the enthalpy method [4, 5], the variational method [6–8], the passive resistance-capacity method [9], numerical methods [10–16], and the Monte Carlo method [17]. Except for a few simple geometries [18], the majority of two-dimensional moving boundary solutions reported in the literature are numerical. Allen and Severn [19], Poots [20], Lazaridis [21], Voller and Cross [5], Crowley [22], Saitoh [23], and Shamsunder and Sparrow [24, 25] presented solutions for solidification of a liquid at freezing temperature in a square prism. A curvilinear coordinate system in conjunction with a finite-difference scheme has been an important feature of the numerical solutions.

In the last two decades, numerous reports [5, 19–23] have indicated that the solidification front in a square prism becomes circular as the solidification front progresses. However, experimental results documented in this paper indicate that many popular phase-change materials do not behave as predicted by the available numerical solutions. Widely-used phase-change materials, *n*-octadecane, and commercial octadecane are selected to show this disagreement. The commercially available octadecane contains isomers of octadecane. A methyl group disrupts the organized crystallization process and the solid exhibits isotropic behavior, an important feature for evaluating an analytical prediction.

In the analytical portion of this study, it is assumed that the speed of the moving boundary is generally slow and the domain of interest is free of any heat sources with rapidly varying temperature. In addition, the effect of the crystallization process and surface kinetics at the interface are neglected. The standard Galerkin method is utilized for computation of the quasi-steady contribution to the solution. The Galerkin method [26] is used because it provides the unique feature of having maximum accuracy at the interface where the heat flux must be calculated. Highly accurate heat flux and other needed derivatives are particularly important when the moving boundary proceeds from a sharp corner. The Galerkin method requires that the moving boundary be defined by a suitable function of time and position. The quasi-steady solution is extended by incorporating the transient contribution corresponding to the first eigenvalue. An approximate integral method which makes use of Galerkin functions is introduced for calculation of this eigenvalue.

MATHEMATICAL FORMULATION

The solution of the diffusion equation in either the solid or the liquid region (Fig. 1) can be decomposed into two parts: a quasi-steady and a transient. This scheme improves the convergence characteristics of the diffusion equation [27]. Although both contributions are transient in nature, the 'transient' in this paper refers to the difference between the general solution and the quasi-steady contribution. If T is the local temperature and T^* represents the local quasi-steady temperature,

† Presently at the University of Al Fateh, Faculty of Engineering, Tripoli, Libya.

NOMENCLATURE

a see Fig. 6
a_i constant
A area
B constant, a parameter of the method
C_p specific heat [kJ kg^{-1} °C^{-1}]
f_i Galerkin function
F auxiliary function
k thermal conductivity [W m^{-1} °C^{-1}]
L slab thickness [m]
$\mathscr{L}$ the latent heat of fusion [kJ kg^{-1}]
M, N number of terms
$\mathbf{n}$ unit vector along outer normal
p constant
$\mathbf{r}$ position vector
$\mathbf{r}_i$ position vector of the hot surface
$\mathbf{r}_m$ position vector of the interface
$\mathbf{r}_0$ position vector of the cold surface
R region
S boundary of region R
t time [s]
T local temperature [°C]
$\hat{T}, T^*$ average and quasi-steady temperatures [°C]
T_i temperature, hot surface [°C]
T_m fusion temperature [°C]
T_o temperature, cold surface [°C]
T_s surface temperature [°C]
V volume
V_r volume ratio of two successive intervals
X, Y, Z Cartesian coordinates.

Greek symbols
α thermal diffusivity [m^2 s^{-1}]
β, γ parameters of the method
θ angular coordinate
λ summation index
ϕ first term in Galerkin function
ρ density [kg m^{-3}].

Subscripts
1 solid
2 liquid
i interface position
j time step
k, l indices
m interface.

then, according to the aforementioned definition

$$T(\mathbf{r}, t) = T^*(\mathbf{r}, t) + [BF(\mathbf{r})/\alpha]\, \mathrm{d}\hat{T}/\mathrm{d}t. \quad (1)$$

The second term on the RHS of equation (1) represents a correction term to the quasi-steady solution which is termed the 'transient' contribution. The function $F(\mathbf{r})$ describes the spatial dependence of temperature T, while $\hat{T}(t)$ is the average temperature in the region under consideration, α is the thermal diffusivity, and B is a parameter to be evaluated later.

The function $T^*(\mathbf{r}, t)$ is to be computed using the Galerkin method with time serving as a parameter. The Galerkin method is selected because, unlike the finite-difference method, it provides smooth temperature distribution and maximum accuracy near the boundary. Once the quasi-steady solution is computed, the Galerkin functions are readily available for computation of the transient contribution. Since the quasi-steady solution includes the nonhomogeneous boundary conditions, the function $F(\mathbf{r})$ must satisfy only a homogeneous set of boundary conditions consistent with those for T.

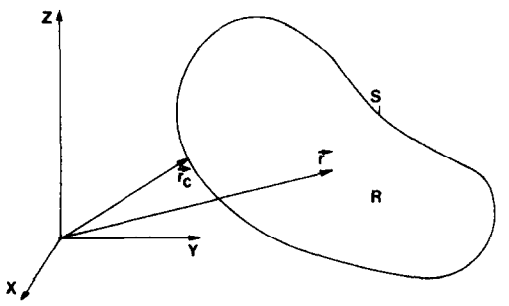

FIG. 1. Schematic of the region R and boundary S.

Any solution of the diffusion equation must satisfy the initial and boundary conditions in addition to the diffusion equation. The uniqueness theorem in the theory of the partial differential equations then guarantees that this solution is unique. However, an approximate solution fails to satisfy all of the aforementioned conditions. In general, the integral solutions satisfy the initial and the boundary conditions while the diffusion equation is satisfied in the integral form. Following the same logic, equation (1) is arranged in a way that satisfies the boundary conditions. The integral form of the diffusion equation in the absence of any internal heat source or sink is

$$\int_S k(\partial T/\partial n)\, \mathrm{d}S = \mathrm{d}(\rho C_p V \hat{T})/\mathrm{d}t \quad (2)$$

where $\mathbf{n}$ is the outward unit vector on surface S, Fig. 1. The constant B in equation (1) can be obtained by substituting equation (1) into (2) and considering that, in accordance with the definition of T^*,

$$\int_S (\partial T^*/\partial n)\, \mathrm{d}S = 0. \quad (3)$$

The value of B obtained in this manner is

$$B = [V + \hat{T}(\mathrm{d}V/\mathrm{d}t)/(\mathrm{d}\hat{T}/\mathrm{d}t)] \Big/ \int_S (\partial F/\partial n)\,\mathrm{d}S \quad (4)$$

In this derivation, the thermal properties in each phase are considered to be independent of temperature and position. Equation (4) ensures that the energy equation in the integral form is satisfied. The remaining unknown in equation (1) is the instantaneous average temperature, $\hat{T}$, which can be computed utilizing the definition of $\hat{T}$; that is

$$\hat{T} = \frac{1}{V}\int_V T\,\mathrm{d}V. \quad (5)$$

Equation (1) can now be substituted in (5) and the result after some rearrangement of the terms is

$$\mathrm{d}\hat{T}/\mathrm{d}t = (\beta - \hat{T})\gamma - (\hat{T}/V)(\mathrm{d}V/\mathrm{d}t) \quad (6)$$

where,

$$\beta = \frac{1}{V}\int_V T^*\,\mathrm{d}V \quad (6a)$$

and

$$\gamma = -\left[\alpha \int_S (\partial F/\partial n)\,\mathrm{d}S\right] \Big/ \int_V F\,\mathrm{d}V. \quad (6b)$$

The second term on the RHS of equation (6) represents the effect of boundary movement on the rate of change of the average temperature. When there is no boundary movement, the term which includes $\mathrm{d}V/\mathrm{d}t$ will vanish. Equation (6) can be integrated analytically between any time t_j and a later time t,

$$\hat{T} = \frac{1}{V}\left[\hat{T}_j V_j + \int_{t_j}^{t} \beta\gamma V \exp\left(\int_{t_j}^{t} \gamma\,\mathrm{d}t\right)\mathrm{d}t\right] \times \exp\left(-\int_{t_j}^{t} \gamma\,\mathrm{d}t\right). \quad (7)$$

It appears that equations (1), (4) and (7) are sufficient for computation of temperature distribution, T. However, the instantaneous configuration of the region under consideration is required. In a moving boundary problem which involves melting or freezing of a phase-change material, the value of $\hat{T}$ and V are interdependent. The interdependency between $\hat{T}$ and V can be defined using the conservation of energy and continuity of temperature at the liquid/solid interface. Therefore, at any point i along the moving boundary the following relation must be satisfied

$$\rho\mathscr{L}(\mathrm{d}r_m/\mathrm{d}t)_i = -k_1[(\partial T_1^*/\partial n_1)_i + (\partial F_1/\partial n_1)_i(\mathrm{d}\hat{T}_1/\mathrm{d}t)B_1/\alpha_1] - k_2[(\partial T_2/\partial n_2)_i + (\partial F_2/\partial n_2)_i(\mathrm{d}\hat{T}_2/\mathrm{d}t)B_2/\alpha_2], \quad (8)$$

where $\mathbf{r}_m$ and $\mathscr{L}$ are the position vector and the latent heat of fusion and $\mathrm{d}\mathbf{r}_m$ is perpendicular to the moving boundary, Fig. 2. In Fig. 2, the subscript 1 refers to solid and 2 refers to liquid. Also, along the moving front, the unit normals $\mathbf{n}_1$ and $\mathbf{n}_2$ have opposite directions. The values of $\mathrm{d}\hat{T}_1/\mathrm{d}t$ and $\mathrm{d}\hat{T}_2/\mathrm{d}t$ are given in equation (6). An appropriate substitution yields the working form of equation (8),

$$\rho\mathscr{L}(\mathrm{d}r_m\,\mathrm{d}t) = -[k_1(\partial T_1^*/\partial n)_i + k_2(\partial T_2^*/\partial n_2)_i] - [G_{1,i}(\beta_1 - \hat{T}_1)\gamma_1 + G_{2,i}(\beta_2 - \hat{T}_2)\gamma_2] \quad (9)$$

where

$$G_{1,i} = \rho_1 C_{p1} V_1 (\partial F_1/\partial n_1)_i \Big/ \int_{S_1} (\partial F_1/\partial n_1)\,\mathrm{d}S_1 \quad (9a)$$

and

$$G_{2,i} = \rho_2 C_{p2} V_2 (\partial F_2/\partial n_2)_i \Big/ \int_{S_2} (\partial F_2/\partial n_2)\,\mathrm{d}S_2. \quad (9b)$$

The first square bracket on the RHS of equation (9) is the contribution of the quasi-steady solution. The second square bracket represents the transient effects not included in the quasi-steady solution.

Equation (9) suggests that the values of $\hat{T}_1$ and $\hat{T}_2$ are needed in order to calculate any change in the values of V_1 and V_2 while V_1 and V_2 are needed to compute $\hat{T}_1$ and $\hat{T}_2$ using equation (7). This gives rise to an iterative procedure. More details of the method of analysis and numerical computations are in the following numerical examples.

NUMERICAL EXAMPLES

Two different moving boundary problems are considered. The availability of solutions in the literature to the problems under consideration is responsible for this selection.

One-dimensional solidification

Consider a liquid region $0 < X < L$ (Fig. 3) initially at temperature $T_i \geqslant T_m$, where T_m is the melting

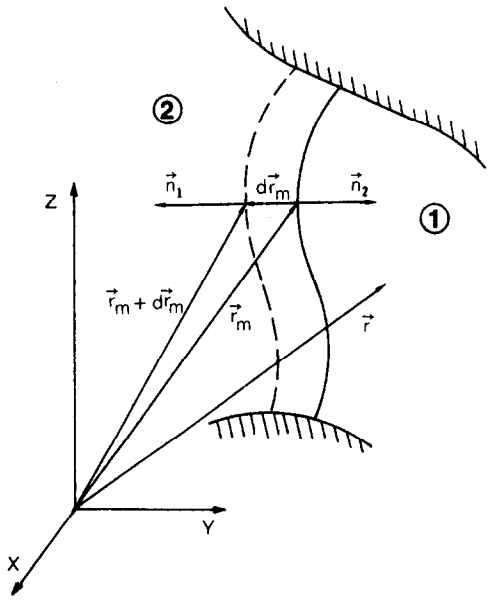

FIG. 2. Schematic of the liquid and solid region.

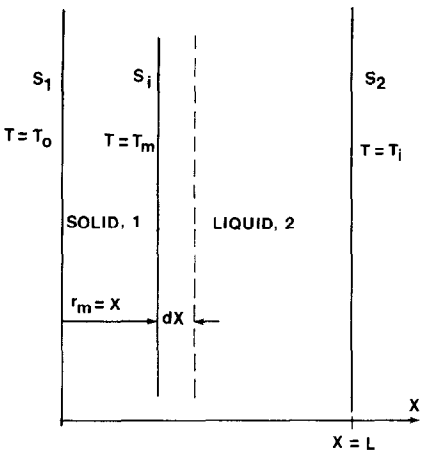

FIG. 3. One-dimensional moving boundary problem.

temperature. When $t > 0$, the temperature of the boundary surface at $X = 0$ is reduced to a constant temperature $T_0 < T_m$. Furthermore, it is assumed that the temperature at $X = L$ remains at temperature T_i. The Galerkin functions for solid and liquid regions are

$$F_1 = X(X - r_m) \tag{10a}$$

and

$$F_2 = (X - r_m)(L - X). \tag{10b}$$

The quasi-steady solutions for this example are well known,

$$T_1^* = T_0 + (T_m - T_0)X/r_m \tag{11a}$$

and

$$T_2^* = T_m + (T_i - T_m)(X - r_m)/(L - r_m). \tag{11b}$$

The values of β_1, β_2, γ_1 and γ_2 are defined using equations (6a) and (6b) as $\beta_1 = (T_0 + T_m)/2$, $\beta_2 = (T_i + T_m)/2$, $\gamma_1 = 12\alpha_1/r_m^2$, and $\gamma_2 = 12\alpha_2/(L - r_m)^2$. Another advantage of this method is that the temperature distribution is computed analytically from equations (1)–(7), hence no numerical instability is expected. However, a finite Δr_m should be selected for the computation of the progress of r_m. The relative size of Δr_m is therefore the only criterion for selecting the size of Δt. Equation (7) for solid and liquid regions when $t_j < t < t_{j+1}$ is written as

$$\hat{T}_{1,j+1} = [\hat{T}_{1,j}V_{r1} - (V_{r1} + 1)\beta_1/2] \exp(-\gamma_1 \Delta t) + (V_{r1} + 1)\beta_1/2 \tag{12a}$$

and

$$\hat{T}_{2,j+1} = [\hat{T}_{2,j}V_{r2} - (V_{r2} + 1)\beta_2/2] \exp(-\gamma_2 \Delta t) + (V_{r2} + 1)\beta_2/2 \tag{12b}$$

where

$$V_{r1} = V_{1,j}/V_{1,j+1} = r_{m,j}/r_{m,j+1} \tag{13a}$$

$$V_{r2} = V_{2,j}/V_{2,j+1} = (L - r_{m,j})/(L - r_{m,j+1}) \tag{13b}$$

$$r_{m,j+1} = r_{m,j} + (\mathrm{d}r_m/\mathrm{d}t) \cdot \Delta t \tag{13c}$$

and

$$\rho \mathscr{L}\, \mathrm{d}r_m/\mathrm{d}t = k_1(6\hat{T}_1 - 2T_0 - 4T_m)/r_m + k_2(6\hat{T}_2 - 2T_i - 4T_m)/(L - r_m). \tag{13d}$$

Equation (13d) is equation (9) written for the one-dimensional problem under consideration. This equation contains singularities at $X = 0$. This singularity can be removed in an elementary manner. For instance, in this example, when $t \to 0$, then $\hat{T}_1 \to (T_m + T_0)/2$ and $\hat{T}_2 \to T_i$. Furthermore, if $T_i = T_m$, $r_{m,1} = \sqrt{2k_1 t(T_m - T_0)/\rho \mathscr{L}}$ when $t < \Delta t$, often used in the numerical study of moving boundary problems during the first time increment.

Following the determination of position and the corresponding time for the first interval, the solution procedure begins for computation of the second interval by assuming Δr_m. For more complicated situations, the value of Δr_m at the onset of each iteration can be computed using the quasi-steady solution. The information available at the earlier steps is then used to calculate the corresponding Δt using equation (13d). Once $r_{m,2}$ and Δt are on hand, equations (12a) and (12b) are used to recalculate $\hat{T}_1$ and $\hat{T}_2$ at time $t + \Delta t$ and obtain a new value of $r_{m,2}$. If two successive values of $r_{m,2}$ do not differ appreciably, the iteration stops; otherwise, the process will continue until convergence is achieved. The values of $r_{m,3}, r_{m,4}, \ldots, r_{m,j}$ are then calculated as a function of time using the aforementioned procedure.

The numerical values for a specific example dealing with the solidification of liquid Glauber salt are computed and presented for two different sets of temperatures in Fig. 4. The thermophysical properties used are

$\rho_1 = 1460\ \mathrm{kg\ m^{-3}}$ $\rho_2 = 1330\ \mathrm{kg\ m^{-3}}$

$k_1 = 1.92\ \mathrm{W\ m^{-1}\ °C^{-1}}$ $k_2 = 3.26\ \mathrm{W\ m^{-1}\ °C^{-1}}$

$C_1 = 0.544\ \mathrm{kJ\ kg^{-1}\ °C^{-1}}$ $C_2 = 1.011\ \mathrm{kJ\ kg^{-1}\ °C^{-1}}$

$\rho \mathscr{L} = 139{,}500\ \mathrm{kJ\ m^{-3}}$ $L = 0.0508\ \mathrm{m}$.

Also, a similar solution, but using a modified boundary-layer integral method, an excellent representative of the experimental data of ref. [3], is plotted in the same figure. The value of r_m calculated by both methods agree remarkably well over the entire range of time used.

The temperatures in the solid and liquid regions are calculated if the information obtained while computing r_m is substituted in equations (12a) and (12b). Figure 5 shows the temperature distribution as a function of time and position within solid and liquid for different sets of boundary conditions. It is observed that the contribution of the transient term is less than 3% and the temperature distribution is a nearly linear function of X in both regions. It is important to note that this method is not being developed for a one-dimensional problem, but it is being considered for more complex problems. The one-dimensional problem is selected mainly to demonstrate the contribution of the transient term in a well-known problem.

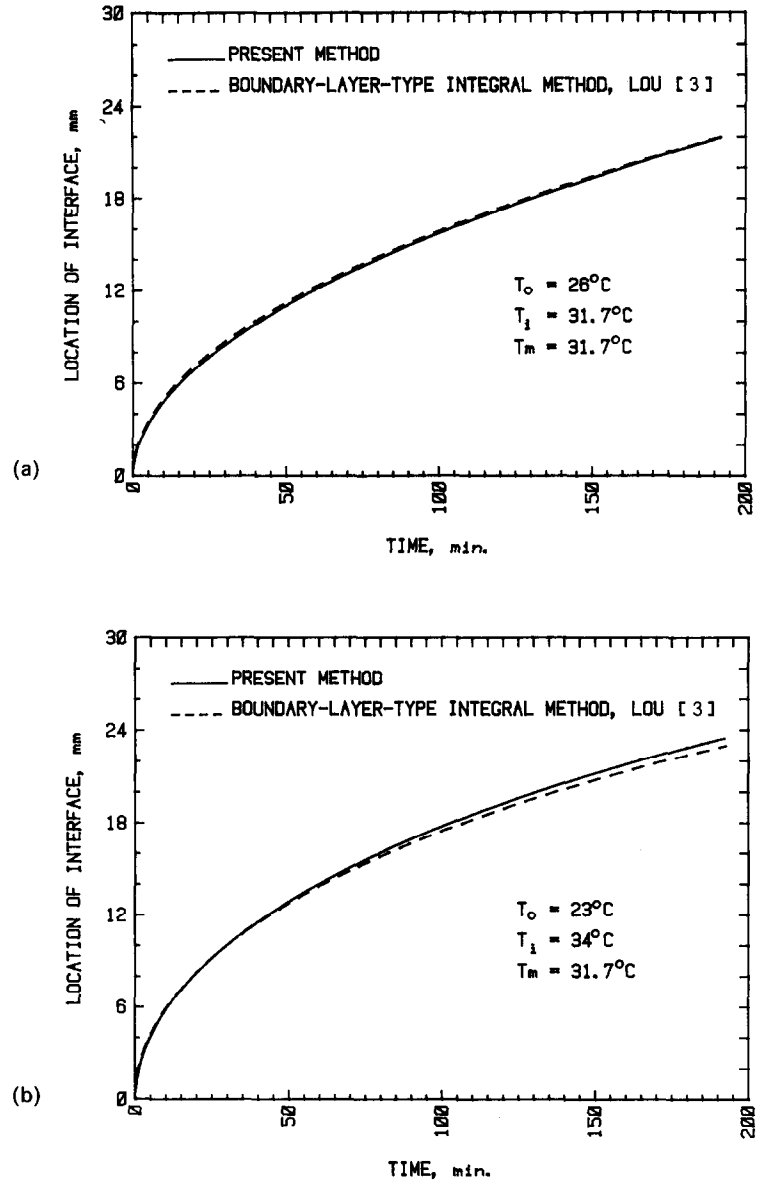

FIG. 4. A comparison of the interface location for this integral method and a boundary-layer-type integral method. (a) $T_i = T_m$, (b) $T_i > T_m$.

Two-dimensional solidification

A two-dimensional problem which has been considered by many investigators deals with solidification of a liquid in an infinitely long square prism. The procedure developed for this example can be equally successful for other two-dimensional configurations. The liquid is assumed to be, initially, at the fusion temperature, T_m, while the outer boundary is maintained at a temperature $T_0 < T_m$. The length of each side is $2a$ (Fig. 6), and the coordinates are selected so that $-a < X < a$ and $-a < Y < a$. Because of geometrical symmetry in both X- and Y-directions, only the portion of solid and liquid located in the first quadrant is selected for this calculation. Inasmuch as the liquid has temperature T_m throughout, only temperature variation in the solid phase will be calculated.

Preliminary to this study, it is essential to define a suitable set of functions which can accurately describe the interface. A severe test for the suitability of any curve-fitting scheme is its ability to accurately describe the external boundary of this square geometry. A least-squares routine using a polynomial in X and Y was unsuccessful. Several other attempts utilizing trigonometric and other type functions did not yield a satisfactory curve fitting of the external surface.

The curve fitting which satisfactorily describes the external surface can best be introduced in cylindrical coordinates. The magnitude of the position vector at the interface is defined as r_m and the angle of inclination

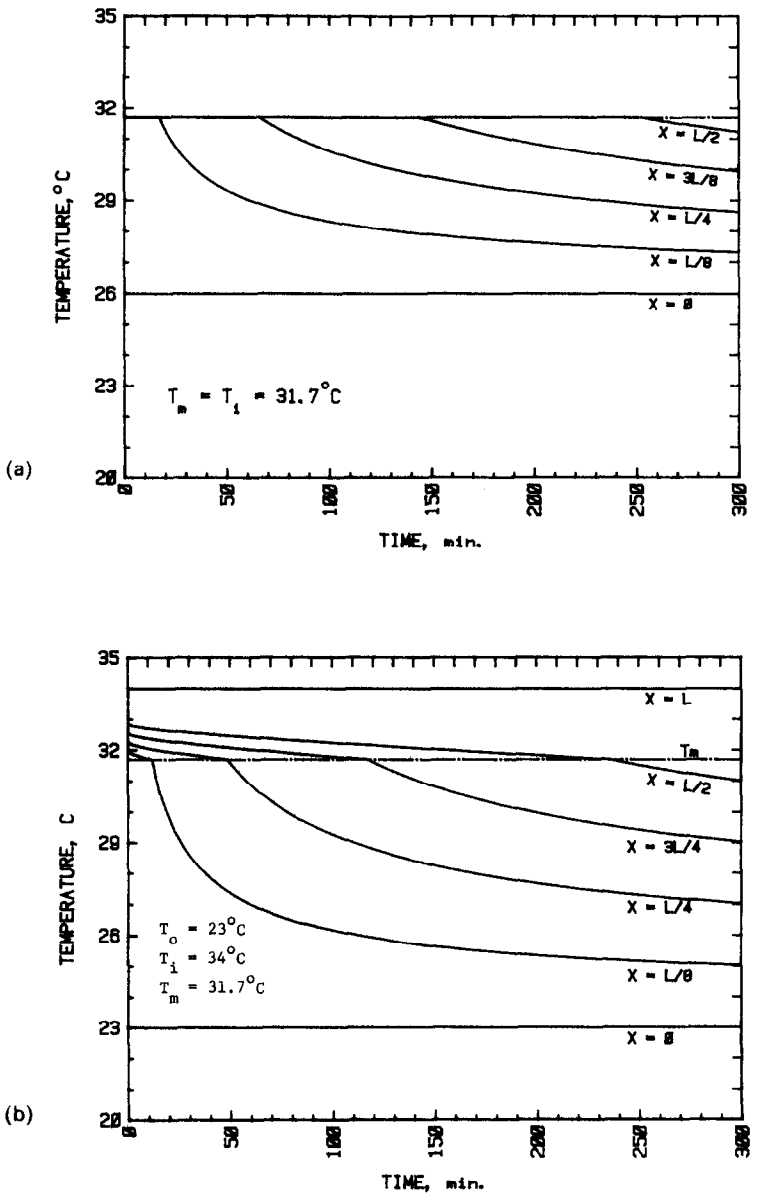

FIG. 5. Transient temperature distribution at various points in the solid and liquid. (a) $T_0 = 26°C$ and $T_i = T_m$, (b) $T_0 = 23°C$ and $T_i > T_m$.

from the X-axis is designated as θ, Fig. 6. The value of r vs θ for the external boundary, that is $X = a$ line and $Y = a$ line, is shown as a set of discrete points on Fig. 7. The functions that describe this type of variation are of exponential form. Among many exponential functions with different combinations, the following form gives the best results,

$$r_m(\theta) = a_1 + (\theta - \pi/4)^2 \sum_{\lambda=2}^{N} a_\lambda \exp\left[-p(\lambda-1)|\theta-\pi/4|\right] \tag{14}$$

where N is the number of terms used for curve fitting. The values of $a_1, a_2, \ldots, a_N$ are to be calculated by a least-squares routine. The absolute-value quantity in the argument of the exponential terms makes this equation symmetric about $\theta = \pi/4$. Among many values of p attempted, $p = 2$ appears to provide the best curve fit solely on the basis of visual observation and standard deviation of the error. Figure 7 is prepared to demonstrate the agreement between this curve-fitting procedure and the outer surface of the solid region which is the boundary of the square region. The representation of the boundary is remarkably accurate and the least-squares curve is smooth. The coefficient a_1 in equation (14) is the radial coordinate of the interface at $\theta = \pi/4$. In the subsequent analysis, r_m will represent the radial coordinate of the solid/liquid interface and r_0 the radial coordinate of the outer boundary. The Galerkin function for a solid region bounded between

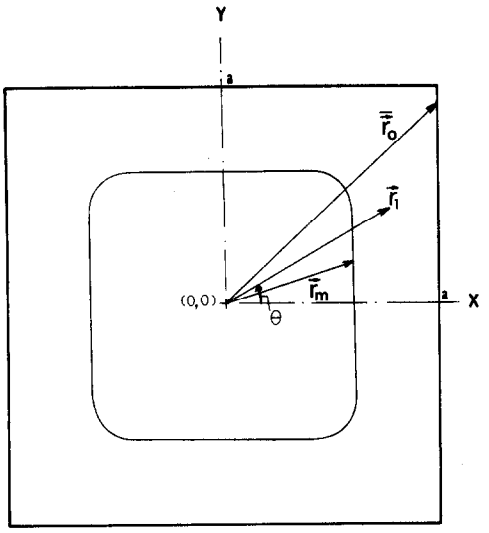

FIG. 6. Schematic of solid and liquid regions in a square prism.

$r = r_m$ and $r = r_0$ lines is

$$\phi = (r - r_m)(r_0 - r) \tag{15}$$

which will be used throughout the following analysis.

The standard Galerkin procedure for calculation of quasi-steady solution of temperature distribution is used. The quasi-steady temperature distribution is governed by the Laplace equation

$$\nabla^2 T_1^* = 0 \tag{16}$$

with boundary conditions $T_1^* = T_m$ when $r = r_m$ and $T_1^* = T_0$ when $r = r_0$. In accordance with the Galerkin procedure [26]

$$\begin{aligned} T_1^* &= g(r, \theta) + \sum_{k=1}^{M} c_k f_k(r, \theta) \\ &= g(r, \theta) + [c_1 + c_2 r + c_3(\theta - \pi/4)^2 + c_4 r^2 + \cdots]\phi \\ &= g(r, \theta) + F(r, \theta) \end{aligned} \tag{17}$$

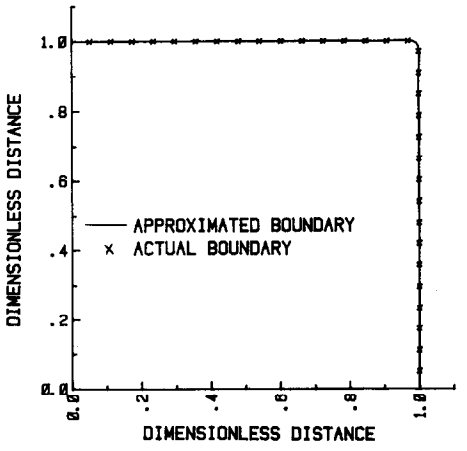

FIG. 7. Least-square computed curve approximating the exterior boundary of the square prism.

wherein $g(r, \theta)$ is an arbitrarily-selected function which satisfies the non-homogeneous boundary conditions and f_k is the product of ϕ and the kth term of the polynomial in r and $(\theta - \pi/4)$, shown in the square bracket of equation (17). The symmetry condition requires that terms with $(\theta - \pi/4)$ to the power of odd exponents to vanish.

Equations (16) and (17) are arranged using the Galerkin procedure as

$$\sum_{k=1}^{M} c_k \int_V f_l \nabla^2 f_k \, dV = -\int_V f_l \nabla^2 g \, dV \tag{18}$$

in which l assumes values of $1, \ldots, M$. The function f belongs to a complete set of functions with continuous first and second derivatives. The evaluation of coefficient c_k requires inversion of a symmetric matrix with the terms

$$\int_V f_l \nabla^2 f_k \, dV = -\int_V \nabla f_l \cdot \nabla f_k \, dV. \tag{18a}$$

The function g is selected so that the non-homogeneous boundary conditions are satisfied

$$g(r, \theta) = T_m + (T_0 - T_m) \ln (r/r_m)/\ln (r_0/r_m). \tag{19}$$

The logarithmic-type function resembles the equation derived for quasi-steady condition in cylindrical solids; however, r_0 and r_m in equation (19) depend on angle θ. Equations (17)–(19) result in computation of coefficients c_k and temperature T_1^*. A different number of terms, M, were used and the results indicate that the payback in terms of accuracy beyond $M = 5$ is small. However, the subsequent data are for $M = 9$.

Initially, the conduction is assumed to be one-dimensional until formation of a predetermined small layer of solid is completed. When there is an established solid layer, the Galerkin method and the numerical procedure described *a priori* are capable of predicting the temperature distribution that results in the computation of the speed of the solidification front. The subsequent numerical results indicate that the quasi-steady solution has a dominating influence and the transient contribution is small.

The methodology of the Galerkin method is well established. Its uniqueness and convergence is documented in ref. [26]. However, the transient contribution is new. A successful transient contribution depends on the manner in which the function $F(\mathbf{r})$ in equation (1) is selected. When the quasi-steady temperature dominates, it is sufficient to use the same $F(\mathbf{r})$ function in (1) as was used for the quasi-steady solution, equation (17). As a consequence, the transient solution will not alter the shape of the solidification front that is predicted by the Galerkin method; it merely offsets the time scale by a small amount which accounts for the finiteness of the specific heat. The second and perhaps more precise method is to consider the F function in equation (1) to be independent of that in (17). In this case, the coefficients $c_1, c_2, \ldots$ in the definition of the F function become the elements of the first eigenvector in the general solution of the diffusion

equation [28]. Additional information on the computation of eigenvectors is included in ref. [29]. In this paper, the function F in equation (17) is selected to be employed in (1) because of several factors. First, the effect of the transient solution in the early stages of solidification may be as large as 5%, it rapidly reduces to below 3% and retains a steady value. In a test case [30], the transient contribution indicated an offset time of approx. 7 min after 4 h of solidification. The second reason is the simplicity of additional steps to predict the offset time without using linear algebra for computation of eigenvectors. Perhaps the most important reason is that it might infer that the transient solution is the cause of a discrepancy between this method and difference methods. It is deemed unwise, at this time, to introduce a new variable into a problem that already features many variables.

Once the quasi-steady solution for T_1^* is in hand, the computation of the progress of the solidification front will begin. Some iteration is required to achieve the final solution. It is logical, as the first step of iteration, to use the quasi-steady solution for T_1^* at discrete points along the interface for computation of dr_m/dt from equation (9) and $\mathbf{r}_{m,j+1}$ from the equation

$$\mathbf{r}_{m,j+1} = \mathbf{r}_{m,j} + \Delta\mathbf{r}_m \qquad (19')$$

where $\Delta r_m = (dr_m/dt)\Delta t$ is the liquid thickness along unit normal to be solidified within time Δt at a given point i. Then equation (7), within the time increment, Δt, is arranged as

$$\hat{T}_{1,j+1} = [\hat{T}_{1,j}V_{r1} - (V_{r1}+1)\beta_1/2]\exp(-\gamma_1\Delta t) + (V_{r1}+1)\beta_1/2 \qquad (20)$$

and it is used for computation of G_1 utilizing equation (9a) and recalculation of $\mathbf{r}_m$. The convergence is usually achieved with only a few iterations.

The maximum travel of the boundary at that point and for a time increment Δt must be less than the radius of curvature at that point. This represents the maximum volume of material which can undergo the change of phase in the neighborhood of a point on the interface with the smallest radius of curvature, Fig. 8.

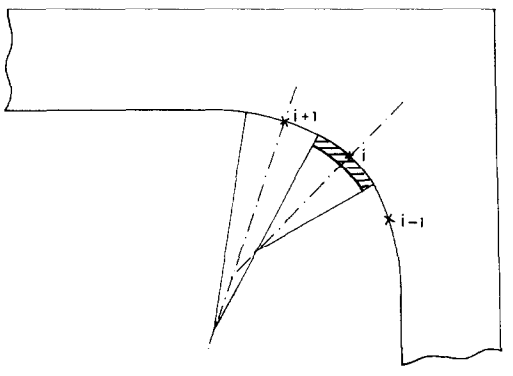

FIG. 8. Schematic of the methodology for calculating volume elements.

For the problem under investigation, the portion of interface with the lowest radius of curvature is at $\theta = \pi/4$. Initially, the quasi-steady solution is used to calculate dr/dt. Since the value of dr at $\theta = \pi/4$ is set in advance in accordance with the requirement described earlier, then the value of Δt is computed. This value of Δt is used to compute Δr at other points along the interface, hence, the first step of interation is complete. The second step of iteration is identical to the first except the values of V_{j+1} and V_j are now in hand and the transient contribution can be included in this analysis. The iteration continues until none of the values of $\hat{T}$ and dr/dt suffer an appreciable change. Thereby, the new position of the interface and the new average temperature, $\hat{T}$, is calculated.

Mashena [30] compared the procedure described herein with the numerical results reported in the literature for freezing of water. The agreement with the analysis of Saitoh [23] along the $\theta = 0$ line is excellent. However, this analysis results in a smaller radius of curvature along the $\theta = \pi/4$ line during later stages of freezing. In addition, the freezing of water [21, 23, 31], indicates that the solidification front becomes circular as it proceeds toward the central portion of the square prism. In addition, Mashena [30] reported that P-116 paraffin wax, a mixture of various hydrocarbons, retains a square-like profile during solidification, unlike water. It is clear that neither water nor paraffin wax are suitable substances for verification of an analytical procedure. The analytical model described in this paper and elsewhere in the literature requires the liquid to remain free from a bulk motion and the solid to be isotropic. In addition to other anomalies not mentioned here, water fails to satisfy these two conditions. Paraffin wax satisfies the above two conditions but it releases its latent heat of fusion over a wide range of temperatures.

In searching for a suitable substance, the authors were able to obtain octadecane rated at 99% pure with a fusion temperature of 28.1°C. The crystallization behavior of this substance is markedly different from that of n-octadecane, but otherwise their behavior is similar. In order to demonstrate that all the required conditions are nearly satisfied, it is of interest to test the solidification of n-octadecane prior to testing octadecane. n-Octadecane is a straight, unbranched chain that can attain a high degree of organization upon solidification. The difference in the solidification behavior of these two substances reveals that the octadecane tested is nearly isotropic in its solid phase.

The n-octadecane is introduced in a container 311 mm in height with a 28.58 × 28.58 mm cross-section. At the outset, the temperature of n-octadecane is brought to nearly the fusion temperature of 28.15°C. The wall temperature of the container is then reduced to 23.65 ±0.15°C. After a preset time, the test is interrupted, the liquid removed, and the solid refrigerated. It is then sectioned and photographed. This process is repeated for other preset times and representative photographs are presented in Fig. 9. The photographs show the

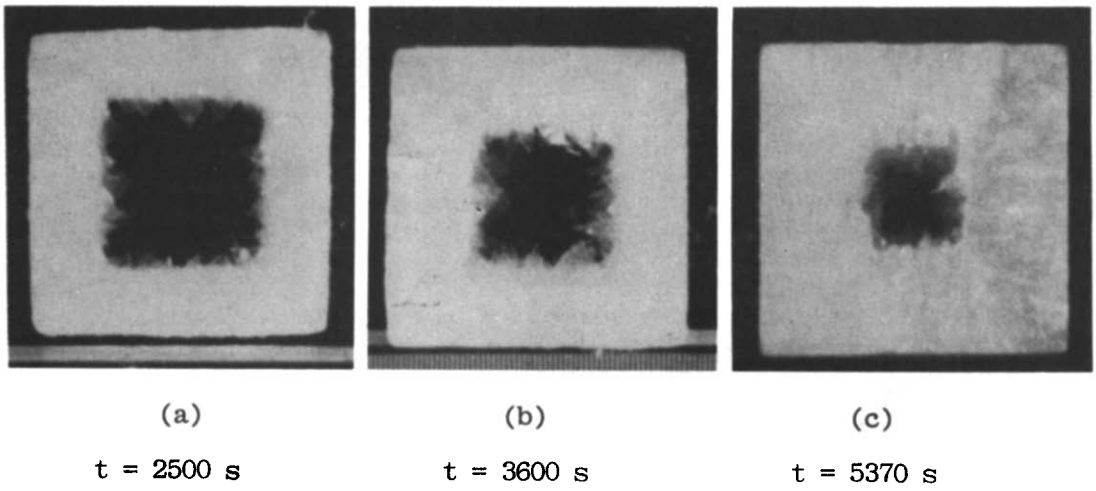

FIG. 9. Solidification of *n*-octadecane in a square prism, fusion temperature 28.15°C.

appearance of needle-like crystals superimposed on a square-like profile with rounded corners. The crystallization is a result of the tendency on *n*-octadecane to attain a high level of organization upon solidification. Following preliminary testing of *n*-octadecane, a commercially available octadecane that contains some octadecane isomers is tested. First, the temperature is measured to be 28.15°C, nearly identical to that for *n*-octadecane. The octadecane is placed in the same container and the test is repeated. Since the bottom of the container is press-fitted with a Plexiglas plate, a light placed beneath the container provides a clear view of the solidification process which is recorded by a camera with an 80-mm macro lens positioned above and looking down into the container. The photographs are shown in Fig. 10. As expected, based on theoretical considerations, the needle-like crystals are absent and the line that separates liquid from solid is quite sharp.

The thermophysical properties of *n*-octadecane [32] are used to analytically predict the instantaneous location of the interface in the above experiments, Fig. 11. There is a remarkable resemblance between the photographs in Figs. 9 and 10 and the analytical results in Fig. 11. The radius of curvature at the corners, $\theta = \pi/4$, in Figs. 9–11 clearly disagrees with similar analyses reported in the literature using discretization techniques. Due to similarity of the molecular structures, this behavior of *n*-octadecane should be reproducible in other straight-chain hydrocarbons suitable for thermal storage applications. Because of this remarkable similarity, Figs. 9–11, it is sufficient to compare the analytical and experimental results along the $\theta = 0$ line. This comparison is shown in Fig. 12. The experimental data for *n*-octadecane are slightly higher than those for octadecane because *n*-octadecane crystals grow perpendicular to the walls of the container and the thermal conductivity is somewhat higher in the direction of crystal growth. Since the fusion temperature of *n*-octadecane and octadecane used in these experiments is nearly the same, the latent heat of fusion is expected to be nearly the same. No change in other thermophysical properties is anticipated. The octadecane data are uncorrected for a slight parallax error estimated to vary between $(0–0.10)r_m(0)/a$. The deviation between octadecane and the analytical prediction is well within this estimated parallax error. The needle-like crystals in Fig. 9 indicate that *n*-octadecane is pure and there is no significant convective flow since a convective flow will prevent formation of the needle-like crystals. The lack of a significant convective flow can be extrapolated to the solidification of octadecane.

The square-like profile of the solidification front may imply that the solidification is one-dimensional. The dashed line in Fig. 12 is prepared based on a one-dimensional assumption. The results indicate that a one-dimensional solution is acceptable during the earlier stages of solidification.

The slower solidification rate of octadecane in comparison with *n*-octadecane is of special importance. It indicates that octadecane has a fixed fusion temperature similar to *n*-octadecane. This point can be further amplified if this analysis is used to predict the solidification of a mixture such as P-116 paraffin wax. The experimental data selected are from ref. [30]. The fusion temperature is 44°C, the temperature of container wall changes with time, and the latent heat is 226 kJ kg^{-1}. The other thermophysical properties are obtained from ref. [33]. Using a two-region approach, only 38% of the latent heat is sufficient to predict the instantaneous location of the interface, Fig. 13. Even a 2% deviation in the value of the latent heat causes significant disagreement between the analysis and the experimental data. This sensitivity of the analysis to the value of the latent heat is responsible for the belief that octadecane behaves as if it has a single fusion temperature. Otherwise, the solidification would have

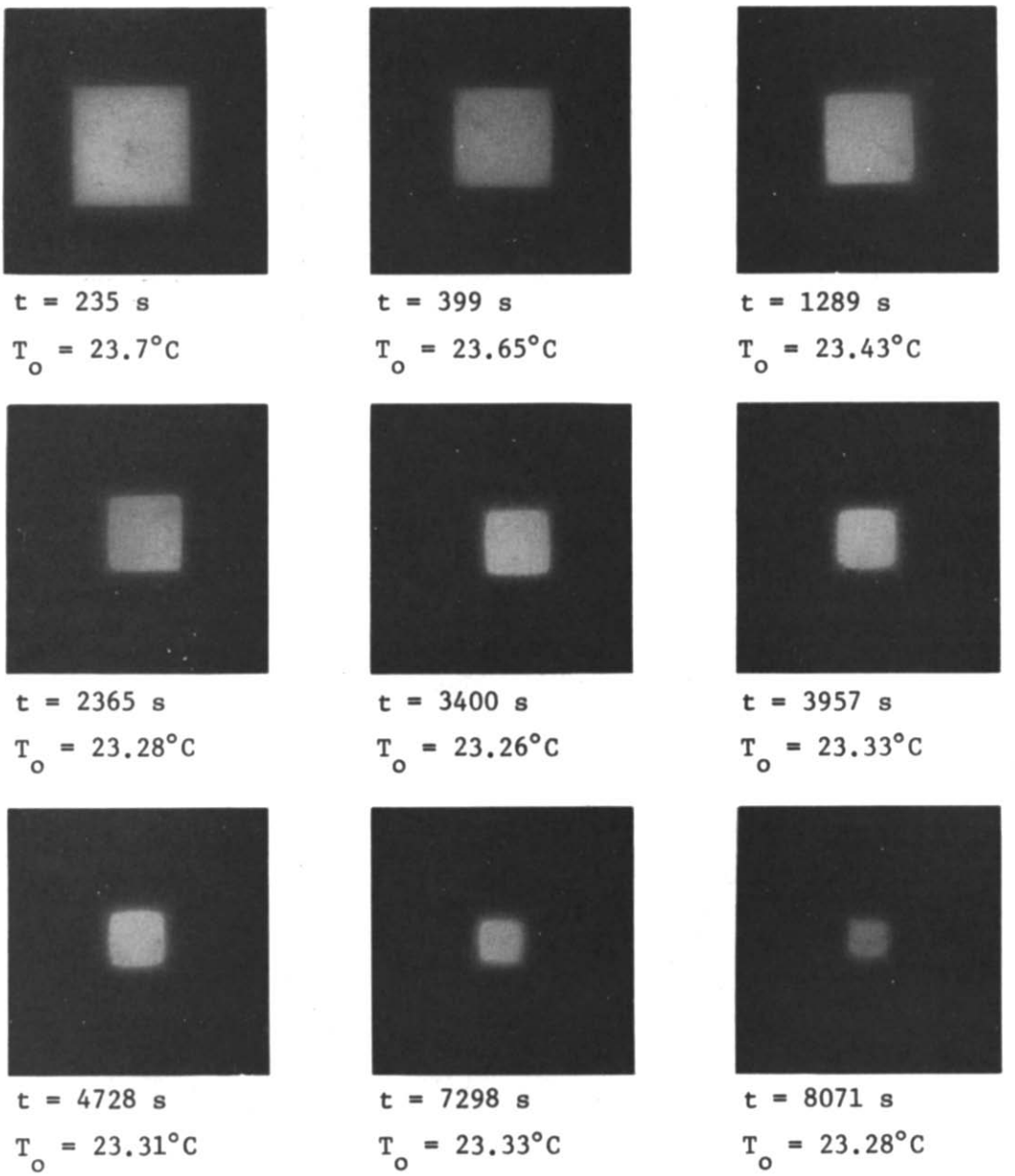

FIG. 10. Solidification of octadecane in a square prism, fusion temperature 28.15°C.

taken place at a much faster rate than predicted by the analysis.

REMARKS

The procedure described in this paper makes use of the Galerkin method to predict solidification problems. The inclusion of transient contribution in the general solution is a simple process. No significant additional effort is required to account for the contribution of directionally-dependent thermal conductivity. Although the numerical examples are for one- and two-dimensional problems, the mathematical derivation is aimed toward three-dimensional applications. The main task for an accurate solution is to seek a suitable function that closely approximates the moving boundary. The region of interest may also be subdivided into smaller regions for convenience of analysis. In this case, the best accuracy can be achieved if function ϕ and its first derivatives are continuous in the entire region.

A proper function for g, equation (19), is essential for a faster convergence. For instance, the accuracy and convergence behavior of the two-dimensional problem is evaluated by assuming the solidification front is circular. Even a single-term Galerkin solution results

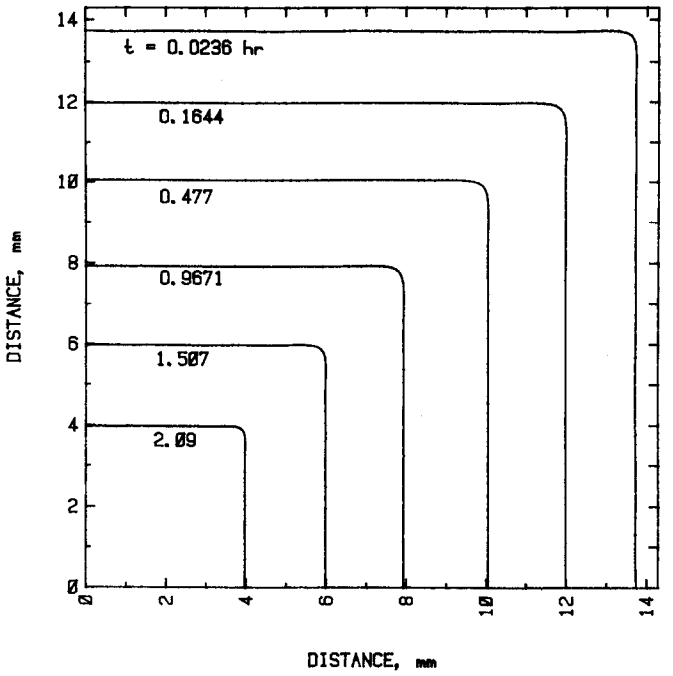

FIG. 11. Computed interface for solidification of octadecane.

in errors less than 10% for most of the region. A six-term solution reveals a high degree of accuracy.

As discussed earlier, there is some disagreement between this method and the discretization methods in the neighborhood of $\theta = \pi/4$ during later stages of solidification. Whenever the physical geometry is discretized, the step size is often too large for accurate resolutions in the neighborhood of $\theta = \pi/4$. The difference between this method and the results using a non-orthogonal transformation is likely caused by an improper use of a mapping function [23]. The boundary function [23]

$$r_0 = 1/\cos(\theta) \quad \text{when} \quad 0 \leqslant \theta \leqslant \pi/4$$

and

$$r_0 = 1/\cos(\pi/2 - \theta) \quad \text{when} \quad \pi/4 \leqslant \theta \leqslant \pi/2$$

causes the mapping function to violate the necessary and sufficient conditions that a mapping function must be a continuous and a single-valued function with continuous first and second derivatives. Since the first derivative of the function r_0 is sectionally continuous, then the mapping becomes singular when $\theta = \pi/4$. The use of a singular second derivative introduces a singularity, analogous to a line heat source, in the transformed diffusion equation, apparently overlooked since the remedial steps are not cited.

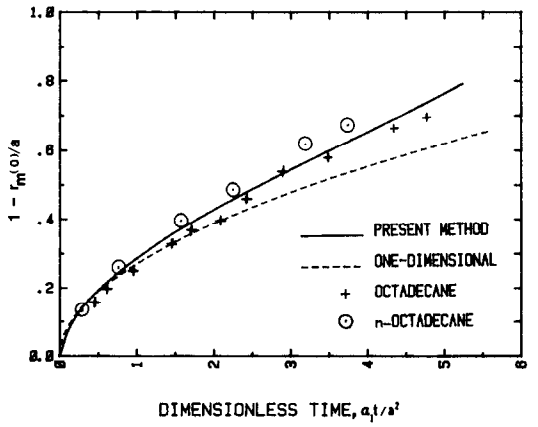

FIG. 12. A comparison between analysis and experimental data for *n*-octadecane and octadecane.

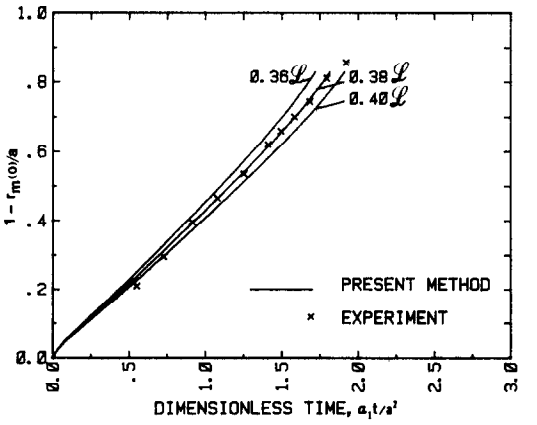

FIG. 13. A comparison between experimental data and analysis for P-116 paraffin wax.

Acknowledgements—This work is supported in part by the National Science Foundation under Grant No. MEA 83-12754. The authors also wish to thank Professors E. M. Sparrow and D. Y. S. Lou, for their many valuable suggestions and Professors R. B. Timmons and Z. A. Schelly who supplied us with octadecane and information on chemical behavior of substances used.

REFERENCES

1. T. R. Goodman, The heat balance integral and its applications to problems involving change of phase, *Trans. Am. Soc. mech. Engrs* **80,** 335–342 (1959).
2. T. R. Goodman and J. J. Shea, The melting of finite slabs, *Trans. Am. Soc. mech. Engrs*, Series B, *J. appl. Mech.* 16–23 (1960).
3. D. Y. S. Lou, Solidification process in a glauber salt mixture, *Sol. Energy* **30,** 115–121 (1983).
4. D. C. Baxter, The fusion times of slabs and cylinders, *Trans. Am. Soc. mech. Engrs*, Series C, *J. Heat Transfer* **84,** 317–326 (1962).
5. V. Voller and M. Cross, Accurate solutions of moving boundary problems using the enthalpy method, *Int. J. Heat Mass Transfer* **24,** 545–555 (1981).
6. T. J. Lardner, Biot's variational principle in heat conduction, *AIAA J.* **1,** 196 (1963).
7. T. J. Lardner, Approximate solutions to phase-change problems, *AIAA J.* **5,** 2079–2080 (1967).
8. A. Prasad and H. C. Agrawal, Biot's variational principle for aerodynamic ablation of melting solids, *AIAA J.* **10,** 325–327 (1972).
9. F. Kreith and F. E. Romie, A study of the thermal diffusion equation with boundary conditions corresponding to solidification or melting of materials initially at the fusion temperature, *Proc. phys. Soc.* **68,** 277–291 (1955).
10. C. Bonacina, G. Comini, A. Fasano and M. Primicerio, Numerical solution to phase change problems, *Int. J. Heat Mass Transfer* **16,** 1825–1832 (1973).
11. F. C. Lockwood, Simple numerical procedure for the digital computer solution of non-linear transient heat conduction with change of phase, *J. Mech. Engng Sci.* **8,** 259–263 (1966).
12. G. S. Lock, J. Gunderson, D. Quon and J. A. Donnelly, A study of one-dimensional ice formation with particular reference to periodic growth and decay, *Int. J. Heat Mass Transfer* **12,** 1343–1352 (1969).
13. L. E. Goodrich, Efficient numerical technique for one-dimensional thermal problems with phase-change, *Int. J. Heat Mass Transfer* **21,** 615–621 (1978).
14. H. G. Landau, Heat conduction in a melting solid, *Q. appl. Math.* **8,** 81–94 (1950).
15. W. D. Murray and F. Landis, Numerical and machine solution of transient heat conduction problems involving melting or freezing, Part I, *Trans. Am. Soc. mech. Engrs*, Series C, *J. Heat Transfer* **79,** 106–112 (1959).
16. P. P. Sharma, M. Rotenberg and S. S. Penner, Phase-change problems with variable surface temperatures, *AIAA J.* **5,** 677–682 (1967).
17. A. Haji-Sheikh and E. M. Sparrow, The solution of heat conduction problems by probability methods, *Trans. Am. Soc. mech. Engrs*, Series C, *J. Heat Transfer* **89,** 121–131 (1967).
18. G. S. Springer and D. R. Olson, Methods of solution of axisymmetric solidification and melting problems, ASME Paper No. 61-Wa-246 (1962).
19. D. N. de G. Allen and R. T. Severn, The application of the relaxation methods to the solution of non-elliptic partial differential equations; III. heat conduction with change of state in two space dimensions, *Q. Jl Mech. appl. Math.* **15,** 339–348 (1962).
20. G. Poots, An approximate treatment of a heat conduction problem involving a two-dimensional solidification front, *Int. J. Heat Mass Transfer* **5,** 339–348 (1962).
21. A. Lazaridis, A numerical solution of the multi-dimensional solidification (or melting) problem, *Int. J. Heat Mass Transfer* **13,** 1459–1477 (1970).
22. A. B. Crowley, Numerical solution of Stefan problems, *Int. J. Heat Mass Transfer* **21,** 215–219 (1978).
23. T. Saitoh, Numerical method for multi-dimensional freezing in arbitrary domains, *Trans. Am. Soc. mech. Engrs*, Series C, *J. Heat Transfer* **100,** 294–299 (1978).
24. N. Shamsundar and E. M. Sparrow, Analysis of multidimensional conduction phase change via the enthalpy method, *Trans. Am. Soc. mech. Engrs*, Series C, *J. Heat Transfer* **97,** 333–340 (1975).
25. N. Shamsundar and E. M. Sparrow, Effect of density change on multidimensional conduction phase change, *Trans. Am. Soc. mech. Engrs*, Series C, *J. Heat Transfer* **98,** 550–557 (1976).
26. L. V. Kantorovich and V. I. Krylov, *Approximate Methods of Higher Analysis.* Wiley, New York (1964).
27. M. N. Ölcer, On the theory of conductive heat transfer in finite regions, *Int. J. Heat Mass Transfer* **7,** 307–314 (1964).
28. A. Haji-Sheikh and M. Mashena, Solution of the diffusion equation using Galerkin functions, ASME paper No. 85-HT-19 (1985).
29. A. Haji-Sheikh, On solution of parabolic partial differential equation. In *Integral Methods in Science and Engineering* (Edited by F. R. Payne, C. C. Corduneanu, A. Haji-Sheikh and T. Huang), pp. 467–479. Hemisphere (1985).
30. M. Mashena, A new integral solution for transient thermal conduction problems. Ph.D. dissertation, University of Texas at Arlington, Arlington, Texas (1984).
31. T. Saitoh, An experimental study of the cylindrical and two-dimensional freezing of water with varying wall temperature, *Tech. Rep. Tohoku Univ.* **41,** 61–72 (1976).
32. A. G. Bathelt, Experimental study of heat transfer during solid–liquid phase change around a horizontal heat source/sink. Ph.D. thesis, Purdue University (1979).
33. A. Haji-Sheikh, J. Eftekhar and D. Y. S. Lou, Some thermophysical properties of paraffin wax as a thermal storage medium, *Prog. Astronaut. Aeronaut.* **86,** 241–253 (1983).

UNE SOLUTION INTEGRALE DES PROBLEMES DE DEPLACEMENT DES LIMITES

Résumé—Une méthode intégrale est présentée, appliquant les fonctions de Galerkin et aboutissant à des solutions de forme fermée pour la distribution des températures dans la phase liquide et solide. Contrairement aux méthods appliquant des suppositions quasi-fermes, la méthode en question retient le résultat de la capacité thermique des solides et des liquides, contribuant de fait à la solution des problèmes relatifs à la température en fonction du temps le long de la limite. La méthode est appliquée aux problèmes de solidification classique à une et deux dimensions en vue de vérifier sa précision. La concordance entre cette méthode et la méthode intégrale des limites à une dimension en vigueur est excellente. Les résulats à deux dimensions pour la géométrie quadrangulaire sont comparés aux données expérimentales obtenues pour l'octodecane.

INTEGRALE LÖSUNG FÜR PROBLEME MIT WANDERNDER GRENZE

Zusammenfassung—Hier wird eine integrale Methode dargestellt, die von Galerkins Funktionen Gebrauch macht und zu einer geschlossenen Lösung der Temperaturverteilung in der flüssigen und festen Phase fürt. Ungleich der Methoden, die von quasi-stabilen Annahmen ausgehen, behält diese Methode die innere Wärmekapazität vom Festen und Flüssigen bei und ist somit brauchbar für probleme, die sich mit zeitabhängiger temperatur entlang der Grenze befassen. Die Methode wird auf klassische ein- und zweidimensionale Erstarrung probleme angewandt, um ihre Genauigkeit zu prüfen. Die Übereinstimmung dieser Methode mit existierenden ein-dimensionalen Grenzschicht-Integralmethode ist asugezeichnet. Die zweidimensionalen Ergebnisse für einen quadratischen Querschmitt werden mit experimentellen Werten verglichen, die mit Oktadekan gewennen wurden.

ИНТЕГРАЛЬНОЕ РЕШЕНИЕ ПРОБЛЕМ ДВИЖЕНИЯ ГРАНИЦ

Аннотация—Интегральный метод предлогает использование функций "Галеркина" и ведет к решениям закрытой формы для температурного распределения в жидкой и твердой фазе. В противоположеность методам применяющии квази-устойчивые предположение, этот метод учитывает результаты внутреннего тепла твердых и жидких веществ, поэтому этот метод способствует разрешению провлем связанных с температурой временной-зависимости вдоль границы. Этот метод применяется при классических одно или двух мерных затвердеваний для проверки их точности. Соответствие между этим двумя методами; м.е., этого метода и существующего одно мерного интегрального слоя границы—превосходно. Двух мерные результаты для квадратной геометрии могут служить для сравнения опытных (экспериментальных) данных полученных для октадекана.